Application of Si-C-O glass-like compounds as negative electrode materials for lithium hybrid capacitors

Hidetaka Konno*, Takashi Kasashima, Kazuhisa Azumi

Division of Materials Chemistry, Graduate School of Engineering, Hokkaido University, Sapporo 060-8628, Japan

Abstract

The Si-C-O glass-like compound (*a*-SiCO) was applied to a negative electrode of a lithium hybrid capacitor (LHC) with activated carbon positive electrodes. The performance as a negative electrode (by a three-electrode system) and LHC (by a two-electrode system) was evaluated in $LiClO_4$ (EC-DEC) and $LiBF_4$ (PC) electrolytes. With *a*-SiCO reversible insertion/extraction of lithium ions at high current densities (0.5-2.0 A g^{-1}) was possible. By prior short-circuiting of the negative electrode with lithium metal in the electrolytes for appropriate periods, the charge/discharge performance of the assembled LHC compared favorably with an electric double layer capacitor (EDLC) made of the activated carbon used for LHC. The cycle performance of the LHC was better but the capacitance was smaller in the $LiBF_4$ (PC) electrolyte than in $LiClO_4$ (EC-DEC) electrolyte. Smaller capacitance is mainly due to lower electric conductivity and higher viscosity of $LiBF_4$ (PC) electrolyte than $LiClO_4$ (EC-DEC) electrolyte. The energy density of the assembled LHC reached a maximum of about three times that of EDLC, with the power density comparable to that of the EDLC.

Keywords: Si-C-O glass-like compound; Lithium hybrid capacitor; Activated carbon

* Corresponding author. Tel.&fax.: +81-11-706-7114.

E-mail address: ko@eng.hokudai.ac.jp (H. Konno)

1. Introduction

Industrial development toward the practical use of hybrid electric vehicles (HV's) and electric vehicles (EV's) calls for electric energy storage devices of high performance, with high energy density, high charging rate, and long life. Rechargeable batteries, such as lithium ion (LIB) and nickel hydride batteries (NHB) are in practical use for HV, but problems with the power density, charging rate, life, costs and so on, remain unsolved, and this exerts a substantial influence on the development of EV. It is well known that electric double layer capacitors (EDLC) have the advantages of high charging rates and good durability, superior to presently available over rechargeable batteries, but has drawbacks in energy density and costs. In particular, activated carbons of high specific surface areas for EDLC are reaching their limits in improvements in volumetric energy density. Of carbon-based materials, those containing hetero-atoms, mainly nitrogen, are considered to be promising due to the large pseudo-capacitance in aqueous electrolytes, but most of them do not give full play to their ability in organic electrolytes [1]. Accordingly, it is rather difficult to expected large energy density for the devices with such materials.

The lithium hybrid capacitor (LHC) is a hybrid device composed of a lithium-doped carbon negative electrode and an activated carbon positive electrode, making it a device which is half LIB and half EDLC [2,3]. Recently, instead of lithium-doped carbon electrodes, conductive polymers [4-7] and transition metal oxides [8-12] have been reported for negative electrodes. With LHC it would be possible to aim at much larger energy densities than EDLC without diminishing the advantages of capacitors over batteries, but the density is not comparable to LIBs which use high capacity negative electrodes, such as crystalline Si, amorphous Si, and others. The negative electrode of a LHC requires a high charging rate as well as high capacity, but the low coulomb efficiency of the first cycle would not be a serious drawback because lithium ion doping is introduced in the assembly process.

We have formed Si-C-O glass-like compound films on exfoliated graphite [13,14], and later synthesized a Si-C-O glass-like compound (abbreviated to *a*-SiCO) with urethane foam templates

[15] as a promising potential electrode material for the negative electrode of LIB: *a*-SiCO showed very large and steady insertion/extraction capacities of lithium ions without potential hysteresis from the second cycle. As briefly described in the previous paper [15], signals of metallic silicon were not distinguished in the XRD pattern and ^{29}Si MAS-NMR spectra of the compound. In addition, cyclic voltammograms in 1 mol dm^{-3} $LiPF_6$ showed a very broad peak at 0.2-1 V vs. Li/Li^+ on the extraction side, but no sharp peaks. Apparently, it is unlikely that the insertion/extraction of lithium ions into *a*-SiCO is based on the alloying/de-alloying with silicon metal, but it has not been possible to elucidate the insertion/extraction mechanism, so far. Additional advantages of *a*-SiCO are that raw materials are inexpensive and not hazardous, and that a synthetic process is simple. A weak point of *a*-SiCO is the low coulomb efficiencies of the first cycle, 60-70%, this is due to the very large insertion capacities which depend on formation temperature of the compound and electrolytes. This irreversible capacity was found to be eliminated by short-circuiting with lithium metal in electrolytes containing lithium ions, that is, by doping lithium ions into the compound [14]. This procedure is very similar to the final step of negative electrode preparation for LHC.

In this study, a *a*-SiCO which showed good performance as a negative electrode material for LIB's [13-15] was assembled into an LHC with activated carbon counter electrodes and the performance was evaluated in two electrolytes by three- and two-electrode systems.

2. Experimental

The *a*-SiCO was synthesized by heat-treatment of the precursor at 1300˚C for 1 h in argon. Details of precursor preparation are described elsewhere [13-16], but briefly, it was obtained by impregnating two types of liquid silicone, $(CH_3)_3SiO\{CH_3(H)SiO\}_mSi(CH_3)_3$ (m≈20, Shin-Etsu Chemical Co. Ltd., KF-99B) and $\{CH_3(CH=CH_2)SiO\}_n$ (n=3-7, Shin-Etsu Chemical Co. Ltd., VC-4), with trace amounts of curing catalyst into urethane foam chips having average pore diameter of about 420 μm, followed

by heating at 200˚C in air, and crushing. It must be noted that urethane foam was used to ensure a homogeneous heat treatment of the cured silicone, and the urethane mostly disappeared by pyrolysis in the inert atmospheres.

The chemical composition of the product was determined in conformity to Japanese industrial standard (JIS R 6124 and Z 2613) by courtesy of Shin-Etsu Chemical Co. Ltd. The specific surface area was measured by nitrogen adsorption at 77 K, and scanning electron microscopy (SEM) was carried out at 5 kV.

The as formed compound was ground with an agate mortar and pestle, and mixed with acetylene black and poly(vinylidene fluoride), 10 mass% each, then fabricated into a working (or negative) electrode by pressing onto a copper foil. A counter (or positive) electrode was made of commercial activated carbon for EDLC (Kuraray Co. Ltd., YP-17) added with acetylene black and poly(tetrafluoroethylene), 10 mass% each, by pressing onto a nickel mesh. A glass cell was used, and working and counter electrodes were set as close as possible using a membrane separator (Asahikasei Chemicals Corp., SV718).

Capacity and cycle performance of the electrode were measured by a three-electrode system with a lithium metal foil, which was used both as a reference electrode and an auxiliary electrode for lithium ion pre-doping, and with a counter (or positive) electrode of activated carbon. Evaluation of the performance as LHC was carried out galvanostatically by a two-electrode system, in which potential changes of both electrodes were monitored using a lithium metal foil as a reference electrode. In a two electrode system, capacitance is based on the total mass of active materials in both electrodes. The electrolyte was 1 mol dm^{-3} $LiClO_4$ (ethylene carbonate (EC) : diethyl carbonate (DEC) = 50:50 vol%) or 1 mol dm^{-3} $LiBF_4$ (propylene carbonate (PC) 100 vol%). The potential range was 0.002-2 V vs. Li/Li^+ for the three-electrode system, and cell voltage 0-3.5 V for the two-electrode system. Current density was 0.5-2 A per gram of active material in the negative electrode. Prior to insertion/extraction measurements, the negative electrode was short-circuited with lithium metal for a

set period, t_{sh}, to pre-dope lithium ions into the electrode and then left on open-circuit for 2 h. All measurements were carried out at room temperature (about 25˚C).

A symmetric EDLC using YP-17 was assembled as a reference device, and the capacitance was measured conventionally in 1 mol dm^{-3} $(C_2H_5)_4NBF_4$ (PC 100%) at 1 A g^{-1} with cell voltage 0-2 V.

3. Results and discussion

3.1. Measured properties of the materials used

Chemical composition of the *a*-SiCO formed at 1300˚C was Si 55, C 28 (free C<2), O 17, N<1, H<0.5, all in mass%. These values are the same as those reported elsewhere [15], except for the free C and N, which were not measured previously. The results indicate that there are practically none of the interactions between carbon and lithium ions that may occur in the case of hard carbons and the nitrogen incorporation from the urethane foam is negligible. The as formed compound looked like fragments of china due to the original shapes of the crushed precursor, and the specific surface area was very small (<100 m^2 g^{-1}).

The specific surface area of activated carbon, YP-17, was 1680 m^2 g^{-1}, a little larger than a catalogue value. To assemble the LHC, the capacitance of the YP-17 as EDLC must be known. The half cell capacitance was measured to be about 100 F g^{-1} in the potential range 2.0-4.0 V vs. Li/Li^+ at 1 A g^{-1} in 1 mol dm^{-3} $LiClO_4$ (EC:DEC=50:50 vol%).

3.2. Performance by a three-electrode system

To use *a*-SiCO as negative electrode of LHC, high rate capability is required. Therefore, the insertion/extraction capacity of *a*-SiCO was measured up to 2.0 A g^{-1} in 1 mol dm^{-3} $LiClO_4$ (EC:DEC=50:50 vol%) using a lithium metal counter electrode without short-circuiting (no pre-doping of lithium ions). Figure 1 shows capacity-potential curves and cycle performance of

a-SiCO formed at 1300˚C at 2.0 A g^{-1}. As reported previously [13-15], the capacity-potential curves of this compound are similar to those of hard carbons, except for the 1st cycle (Fig. 1 (a)). The irreversible capacity of the 1st cycle is very large but the coulomb efficiency becomes nearly 100% within 10 cycles (Fig. 1 (b)). The reversible capacities are 310 mA h g^{-1} at the 10th cycle and gradually decrease in further cycles, but are still 230 mA h g^{-1} at the 200th cycle. The average extraction capacities of the initial 10 cycles were 780 mA h g^{-1} at 50 mA g^{-1}, 580 mA h g^{-1} at 0.5 A g^{-1}, 430 mA h g^{-1} a 1.0 A g^{-1}, and 360 mA h g^{-1} at 1.5 A g^{-1}. Thus, the capacity decreased with increasing current density but the results suggest that this compound is potentially useful for LHC applications.

Figure 2 shows the performance of *a*-SiCO using an activated carbon counter electrode after short-circuiting for t_{sh}= 4 min followed by 2 h on open-circuit under the same conditions as in Fig. 1. Here, based on the capacitance of YP-17 measured above and the data in Fig. 1, sufficiently large amounts (more than five times in mass) of YP-17 were used for the counter electrode. The first insertion curve starts around 0.7 V vs. Li/Li^+, which is consequent on lithium ion doping (Fig. 2 (a)). When a lithium metal counter electrode was used in separate measurements, this starting potential was lower than 0.5 V vs. Li/Li^+. The only possible explanation is a difference in the counter electrode. There is a possibility that the active carbon counter electrode contacting to the working electrode through a membrane separator may reduce the activity of lithium ion in the thin gap by adsorption, because the counter electrode was covering the working electrode completely. When the short-circuiting time is sufficiently long, diffusion of lithium ions from the bulk electrolyte may compensate this phenomena, but in the case of Fig. 2, it was 4 min. The result suggests that t_{sh} should be longer as in the previous experiments [14], and the irreversible capacity of the 1st cycle disappears by short-circuiting. In Fig. 2(b), the capacitance in F g^{-1} is also indicated by converting the capacity in mA h g^{-1} using the potential range, 0.002-2.0 V vs. Li/Li^+. Though the capacities (200 mA h g^{-1} at the 10th cycle and 180 mA h g^{-1} at the 200th cycle) are lower than those shown in Fig. 1 (b), cycle performance is much better. The capacities at 1.0 A g^{-1} under the same assembly were 430 mA h g^{-1} at

the 10th cycle, and 390 mA h g^{-1} at the 100th cycle. The improved cycle performance may be due to lithium ion doping which homogenizes the electrode surface somewhat.

3.3. Performance by a two-electrode system

At 1.0 A g^{-1}, the cell capacitance of a symmetric EDLC using YP-17 was 22 F g^{-1} and the energy density was 11 W h kg^{-1} in 1 mol dm^{-3} $(C_2H_5)_4NBF_4$ (PC 100%). These values are as would be expected from the half cell capacitance measured in 1 mol dm^{-3} $LiClO_4$ (EC:DEC=50:50 vol%), about 100 F g^{-1}. The average power density during the first 50 cycles was 490 W kg^{-1} and the cycle performance was flat.

In the case of LHC, which is an asymmetric capacitor, the cell capacitance, C_{cell}, in F g^{-1} is given by

$$(C_{cell}W_{cell})^{-1} = (C_+W_+)^{-1} + (C_-W_-)^{-1} \quad (1)$$

where W is the mass of active material in g, $W_{cell}=W_++W_-$, and the suffixes, + and -, indicate positive and negative electrodes, respectively. According to Eq. (1), the theoretical cell capacitances as a function of the mass ratio, $W_+/(W_++W_-)$, were calculated using the half cell capacitances of YP-17 and *a*-SiCO. As shown in Fig. 3, the maximum cell capacitance is achieved in the range $W_+/(W_++W_-)$=0.72-0.77, whereas it appears at $W_+/(W_++W_-)$=0.5 for the symmetric EDLC using YP-17. Based on this calculation, the positive to negative electrode mass ratio for LHC was set as 3 to 1 in the following.

The cell performance of an assembled LHC using *a*-SiCO in different electrolytes is shown in Figs. 4-6. The t_{sh} was 60 min, except for the additional data in Fig. 6 (t_{sh}=30 min). Changes in the cell voltage and electrode potentials at 2.0 A g^{-1} in both electrolytes are shown in Fig. 4, where the cycles between the 2nd and 200th are omitted for simplicity but they fall between the two. It should be noted again that the current density is based on the mass of *a*-SiCO and the cell capacitance on the total mass of both electrodes (excluding acetylene black and binders). The cell voltage is the difference between the potentials of the positive and negative electrodes. The starting potentials of the negative

electrode (1st cycle in Fig. 4) are lower than 0.5 V vs. Li/Li^+ due to the pre-doping of lithium ions, leading to a starting cell voltage of about 2.8 V in both electrolytes. The triangular voltage change begins from the 2nd cycle. It is distinctive that the charging curves are upward convex, while the discharging curves are nearly linear. This arises mainly from the potential change at the negative electrode, a characteristic of *a*-SiCO (cf. Figs. 1(a) and 2(a), also). The linearity of the discharging curve became better with increasing number of cycles. *IR* drops observed at both electrodes stem largely from contact resistance between the active materials and the substrates, but they are larger in $LiBF_4$ (PC) electrolyte than in $LiClO_4$ (EC-DEC) electrolyte. The fairly large *IR* drop at the positive electrode in $LiBF_4$ electrolyte may not be due to the conductivity of the electrode, because the positive electrode without adding acetylene black showed similar results to Fig. 4 in both electrolytes. Instead it is mainly ascribed to a lower electric conductivity and higher viscosity of $LiBF_4$ (PC) electrolyte than $LiClO_4$ (EC-DEC) electrolyte [17-19]. For the same reason, the cell capacitance in $LiBF_4$ (PC) electrolyte is smaller than in $LiClO_4$ (EC-DEC) electrolyte, even though the BF_4^- ion is smaller than the ClO_4^- ion.

Figure 5 shows the cycle performance of LHC based on the data shown in Fig. 4, where the contribution of the *IR* drop is corrected. In $LiClO_4$ (EC-DEC) electrolyte, cell capacitance decreases initially but the decrease between the 50th and 200th cycles is only 5.4% (38.6 —> 36.5 F g^{-1}). The initial decrease in cell capacitance is due to the negative electrode (Fig. 2(b)). In $LiBF_4$ (PC) electrolyte, however, after the initial decrease cell capacitance gradually increases to a steady value of about 33-34 F g^{-1}. This kind of change was not marked at lower current densities but actually the cell capacitance increased with increasing number of cycles. It is possible that this change is caused by the $LiBF_4$ (PC) electrolyte, but supporting data are necessary to give a definite explanation.

The cell capacitances at the 50th discharge are shown as a function of current density in Fig. 6 as the efficiency at this cycle is nearly 100%. The rate capability in $LiClO_4$ (EC-DEC) electrolyte is good, independent of t_{sh}, and the cell capacitances for t_{sh}=60 min are much larger than that of EDLC using

YP-17. Figure 7 shows that when t_{sh} is shorter, the potential of the negative electrode during the discharge rises quickly and the end potential becomes higher after relatively small number of cycles, leading to a quick drop in cell voltage in the latter half of discharging (50th cycle in Fig. 7). This is a consequence of insufficient pre-doping with lithium ions, and shows in the decrease in cell capacitance (t_{sh}=30 min in Fig. 6). A similar indication is observed for t_{sh}=60 min in Fig. 4, but it is essential to ensure an appropriate t_{sh} for higher capacitance and long life. When t_{sh} was much longer, 5 or 10 h, the electrode potential at the end of the discharge became lower than 1 V vs. Li/Li^+, which brought about the formation of solid electrolyte interphase (SEI) on the activated carbon and/or insertion of lithium ions into the positive electrode. Thus, an excess of pre-doping with lithium ions may give rise to adverse effects on the cycle performance of LHC. Practically, capacitors are not discharged to 0 V, and by setting the cutoff voltage at around 1 V the above problem is avoided.

One noteworthy conclusion of Figs. 4-6 is that this LHC can be operated in electrolytes containing PC: improvement of performance would be likely when blending with other solvents such as dimethyl carbonate (DMC), DEC, and others.

Figure 8 is a Ragone plot for the present LHC using the data at the 50th discharge. The energy density and the power density are based on the mass of the active materials, and this plot should not be compared directly with that for actual devices. Actually, the energy density of EDLC using YP-17 shown in Fig. 8 is three times the values of commercial EDLC. It is evident that the energy density of LHC is much larger than that of EDLC, though the power density is similar to that of commercial EDLC, 200-800 W kg^{-1}. The LHC with t_{sh}=60 min in $LiClO_4$ (EC-DEC) electrolyte indicates 74 (at 0.5 A g^{-1}) to 59 (at 2.0 A g^{-1}) W h kg^{-1}. This large energy density results from increases in the cell capacitance (Fig. 6), but is partly owing to the 3.5 V cell voltage, which is realized by the low potential of the negative electrode. The energy density of EDLC using YP-17 may be increased by raising the cell voltage, but due to the rise in the potential of the positive electrode the increment will be limited to tens of percent. In this respect pre-doping with lithium ion would be advantageous. At

any rate, the life must be evaluated by extended cycle tests.

4. Conclusions

In this study, *a*-SiCO, which showed good performance as a negative electrode material for lithium ion batteries (LIB) was applied to a negative electrode of a lithium hybrid capacitor (LHC) with activated carbon (YP-17) positive electrodes. The performance as a negative electrode (by a three-electrode system) and LHC (by a two-electrode system) was evaluated in 1 mol dm^{-3} $LiClO_4$ (EC:DEC=50:50 vol%) and 1 mol dm^{-3} $LiBF_4$ (PC 100%). The following conclusions may be made:

(1) The *a*-SiCO was capable of reversible insertion/extraction of lithium ions at high current densities with activated carbon counter electrodes.

(2) It was confirmed that the pre-doping of lithium ions into the negative electrode, by short-circuiting, with lithium metal in the electrolytes eliminates the irreversible capacity of the 1st cycle. The pre-doping level can be estimated by monitoring the electrode potential.

(3) The charge/discharge performance of the assembled LHC compared favorably with EDLC. It is, however, essential to allow an appropriate short-circuiting time to achieve higher capacitance and a longer life.

(4) In the $LiBF_4$ (PC) electrolyte, the cycle performance of LHC was better but the capacitance was smaller than in $LiClO_4$ (EC-DEC) electrolyte. The smaller capacitance is mainly due to the lower electric conductivity and larger viscosity of $LiBF_4$ (PC) electrolyte (larger than $LiClO_4$ (EC-DEC) electrolyte), and this issue may be improved by blending suitable solvents, such as DMC, DEC, and others.

(5) The energy density of the assembled LHC reached about three times that of EDLC using YP-17, though the power density was comparable to that of EDLC.

(6) The *a*-SiCO might be one of the potential electrode materials for LHC. At any rate, the life must

be evaluated by extended cycle tests.

Acknowledgements

A part of the present work was supported by the Grant-in-Aid for Scientific Research (B) from JSPS (No.18350102).

References

[1] D. Hulicova, M. Kodama, H. Hatori, Chem. Mater. 18 (2006) 2318-2326.

[2] Japanese published unexamined application 08-107048 (1996), 09-55342 (1997).

[3] A. Yoshino, T. Tsubata, M. Shimoyamada, H. Satake, Y. Okano, S. Mori, S. Yata, J. Electrochem. Soc. 151 (2004) A2180-2182.

[4] A.D. Fabio, A. Giorgi, M. Mastragostino, F. Soavi, J. Electrochem. Soc. 148 (2001) A845-A850.

[5] A. Laforgue, P. Simon, J.F. Fauvarque, J.F. Sarrau, P. Lailler, J. Electrochem.Soc. 148 (2001) A1130-A1134.

[6] A. Laforgue, P. Simon, J.F. Fauvarque, M. Mastragostino, F. Soavi, J.F. Sarrau, P. Lailler, M. Conte, E. Rossi, S. Saguatti, J. Electrochem. Soc. 150 (2003) A645-A651.

[7] D. Villers, D. Jobin, C. Soucy, D. Cossement, R. Chahine, L. Breau, D.Bélanger, J. Electrochem. Soc. 150 (2003) A747-A752.

[8] G.G. Amatucci, F. Badway, A.D. Pasquier, T. Zheng, J. Electrochem. Soc.148 (2001) A930-A939.

[9] A.D. Pasquier, A. Laforgue, P. Simon, G.G. Amatucci, J.F. Fauvarque, J. Electrochem. Soc. 149 (2002) A302-A306.

[10] W. Dong, J.S. Sakamoto, B. Dunn, Sci. Tech. Adv. Mater. 4 (2003) 3-11.

[11] T. Brousse, R. Marchand, P.-L. Taberna, P. Simon, J. Power Sources 158 (2006) 571–577.

[12] T. Brousse, P-L. Taberna , O. Crosnier, R. Dugas, P. Guillemet, Y. Scudeller, Y. Zhou, F. Favier,

D. Bélanger, P. Simon, J. Power Sources 173 (2007) 633-641

[13] H. Konno, T. Morishita, S. Sato, H. Habazaki, M. Inagaki, Carbon 43 (2005) 1111-1114.

[14] H. Konno, T. Morishita, C-Y. Wan, T. Kasashima, H. Habazaki, M. Inagaki, Carbon 45 (2007) 477-483.

[15] H. Konno, T. Morishita, S. Sato, H. Habazaki, M. Inagaki, ECS Trans. 1[4] (2006) 509-514.

[16] H. Konno, T. Kinomura, H. Habazaki, M. Aramata, Carbon 42 (2004) 737-744.

[17] M. Ishikawa, M. Morita, M. Asao, Y. Matsuda, J. Electrochem. Soc. 141 (5) (1994) 1105-1108.

[18] D. Brouillette, G. Perron, J.E. Desnoyers, Electrochim. Acta 44 (1999) 4721-4742.

[19] K. Xu, Chem. Rev. 104 (2004) 4303-4417.

Figure captions

Fig. 1 (a) Capacity-potential curves and (b) cycle performance of *a*-SiCO at 2.0 A g^{-1} in 1 mol dm^{-3} $LiClO_4$ (EC: DEC=50:50 vol%) in a three electrode system using a lithium metal counter electrode (without short-circuiting).

Fig. 2 The performance *a*-SiCO using an activated carbon counter electrode after short-circuiting for t_{sh} = 4 min followed by 2 h open-circuiting under the same condition with Fig. 1.

Fig. 3 Calculated theoretical cell capacitance using C_+=100 F g^{-1}, $C_-(1)$ = 630 F g^{-1} (350 mA h g^{-1}), $C_-(2)$ = 720 F g^{-1} (400 mA h g^{-1}), $C_-(3)$= 900 F g^{-1} (500 mA h g^{-1}), and $C_-(4)$ = 1080 F g^{-1} (600 mA h g^{-1}). Capacitances in F g^{-1} are calculated from the capacities in mA h g^{-1} using a potential range of 0.002-2.0 V.

Fig. 4 Changes in the cell voltage of LHC and electrode potentials at 2.0 A g^{-1} in different electrolytes: t_{sh}=60 min. The negative electrode was *a*-SiCO and the positive electrode YP-17: W_-/W_+=1/3.

Fig. 5 Cycle performance of LHC under the same condition as in Fig. 4. Filled symbols are charging and open symbols discharging.

Fig. 6 Rate capability of LHC: cell capacitances are the discharge capacitance at the 50th cycle. The negative electrode was *a*-SiCO and the positive electrode YP-17: W_-/W_+=1/3.

Fig. 7 Changes in the cell voltage of the LHC and electrode potentials at 0.5 A g^{-1} in $LiClO_4$ (EC-DEC) electrolyte: t_{sh}=30 min. Electrodes are the same as those in Fig. 4.

Fig. 8 Ragone plot of the present LHC. Experimental conditions and symbols are the same as those in Fig. 6.

Fig. 1

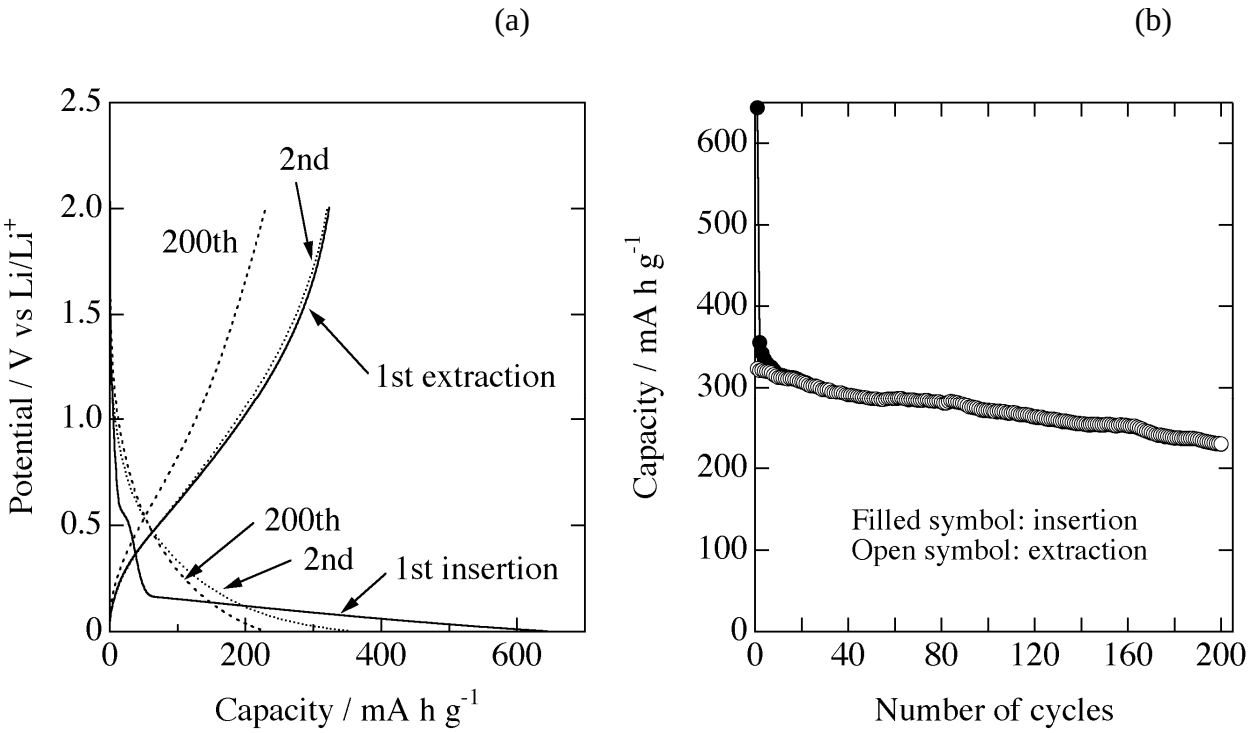
(a)
(b)
2.5
2.0
1.5
1.0
0.5
0
Potential / V vs Li/Li+
2nd
200th
1st extraction
200th
2nd
1st insertion
0
200
400
600
Capacity / mA h g-1
600
500
400
300
200
100
0
Capacity / mA h g-1
Filled symbol: insertion
Open symbol: extraction
0
40
80
120
160
200
Number of cycles

Fig. 2

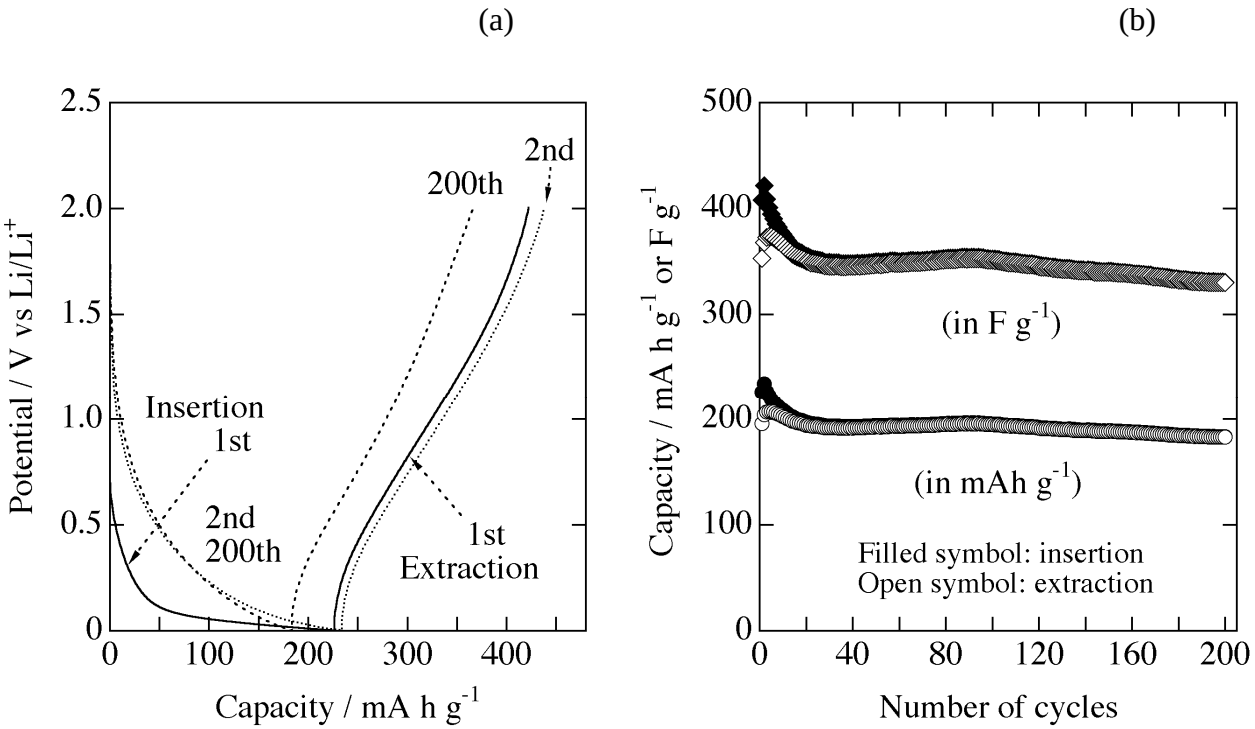
(a)
(b)
Potential / V vs Li/Li+
Capacity / mA h g-1
Insertion
1st
2nd
200th
200th
2nd
1st
Extraction
Capacity / mA h g-1 or F g-1
(in F g-1)
(in mAh g-1)
Filled symbol: insertion
Open symbol: extraction
Number of cycles

Fig. 3

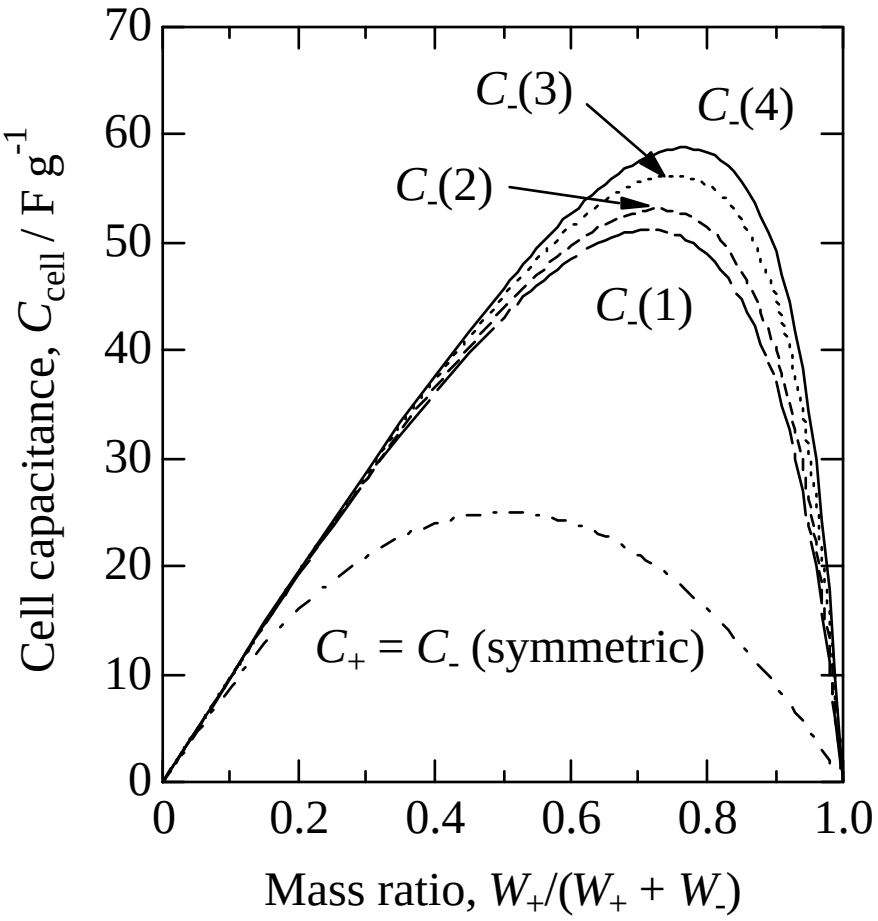
70
60
50
40
30
20
10
0
0
0.2
0.4
0.6
0.8
1.0
Cell capacitance, C_{cell} / F g^{-1}
Mass ratio, $W_+/(W_+ + W_-)$
$C_-(3)$
$C_-(4)$
$C_-(2)$
$C_-(1)$
$C_+ = C_-$ (symmetric)

Fig. 4

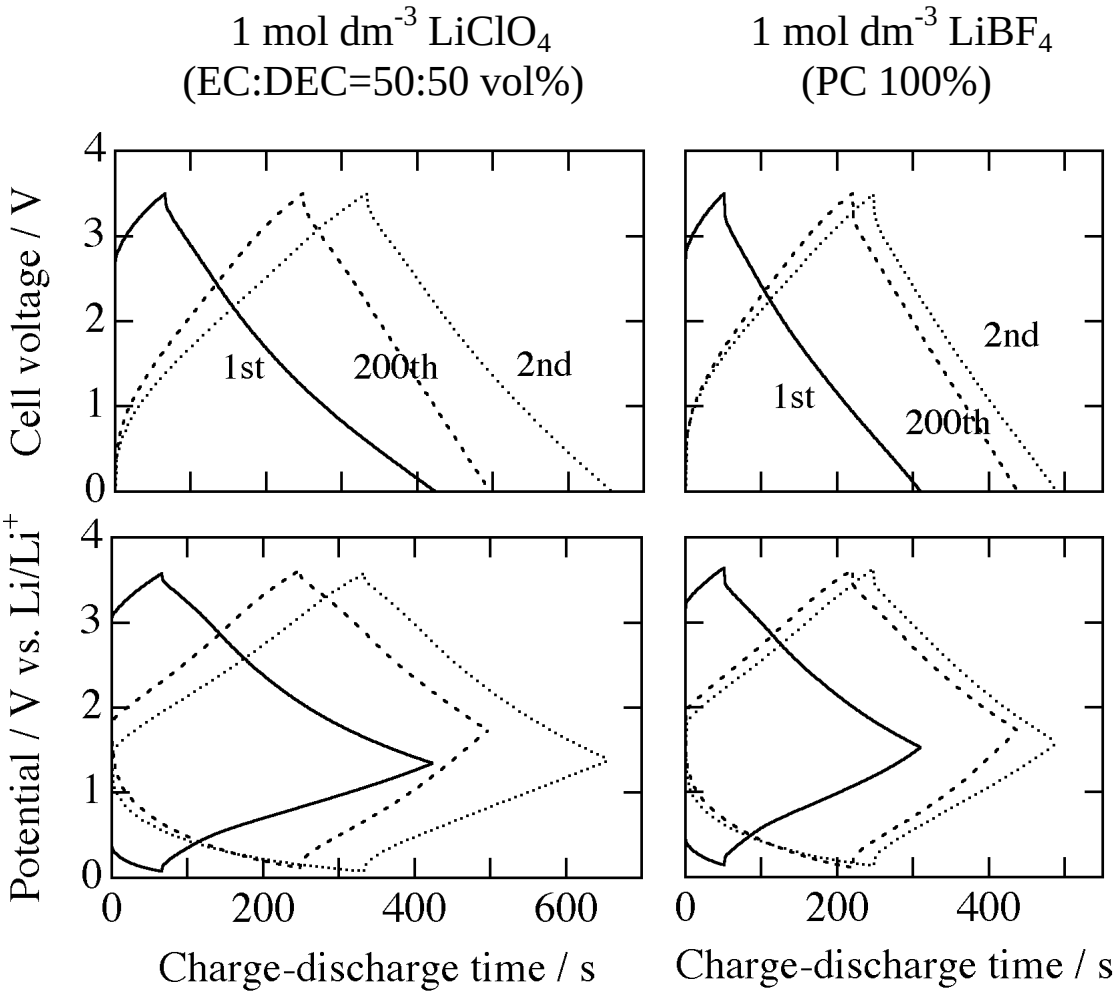
1 mol dm-3 LiClO4
(EC:DEC=50:50 vol%)
1 mol dm-3 LiBF4
(PC 100%)
Cell voltage / V
Potential / V vs. Li/Li+
1st
200th
2nd
2nd
1st
200th
0
1
2
3
4
0
200
400
600
Charge-discharge time / s
Charge-discharge time / s

Fig. 5

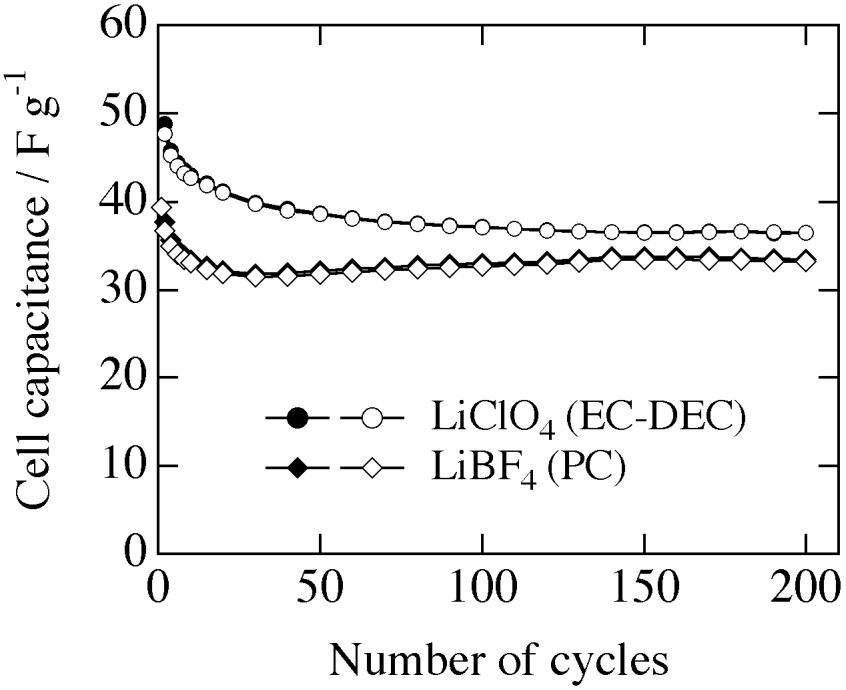
60
50
40
30
20
10
0
0
50
100
150
200
Cell capacitance / F g-1
Number of cycles
LiClO4 (EC-DEC)
LiBF4 (PC)

Fig. 6

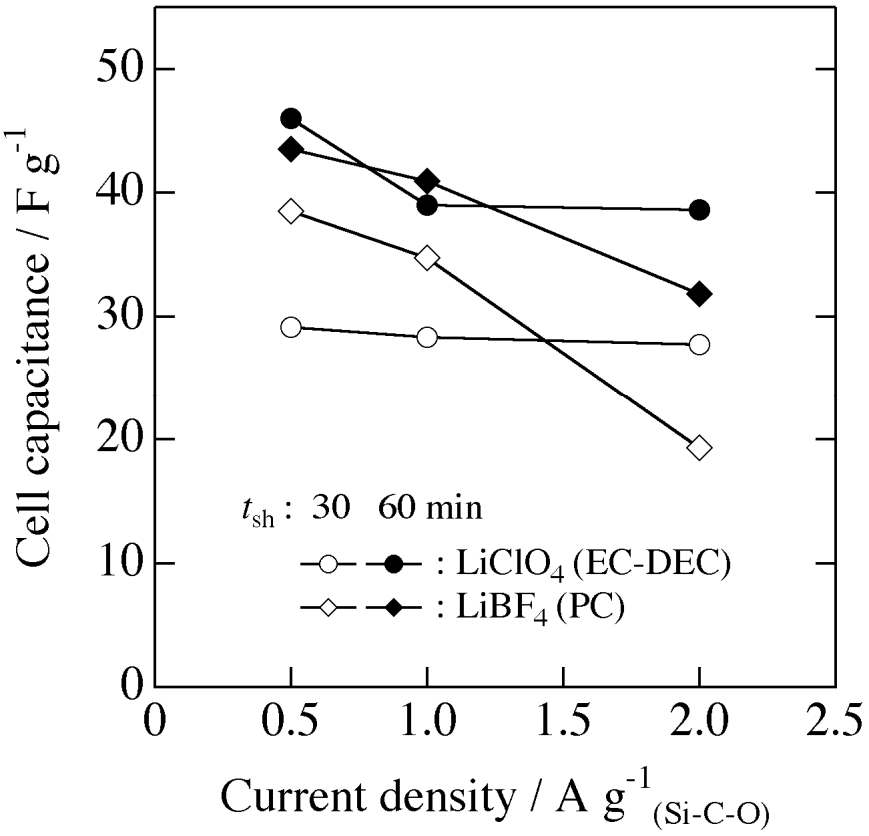
Cell capacitance / F g-1
50
40
30
20
10
0
0
0.5
1.0
1.5
2.0
2.5
Current density / A g-1 (Si-C-O)
tsh : 30 60 min
: LiClO4 (EC-DEC)
: LiBF4 (PC)

Fig. 7

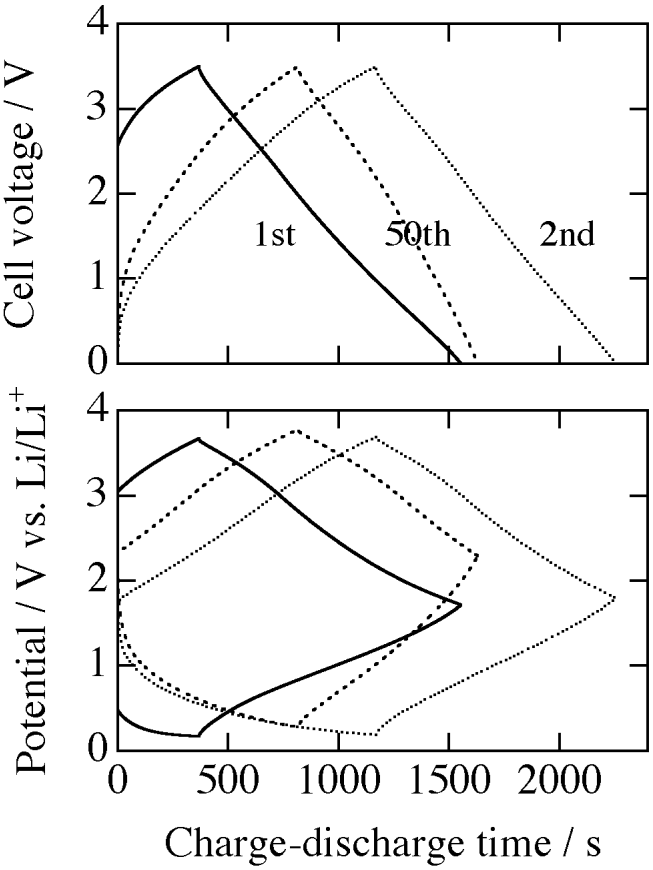
Cell voltage / V
Potential / V vs. Li/Li+
1st
50th
2nd
0
1
2
3
4
0
500
1000
1500
2000
Charge-discharge time / s

Fig. 8

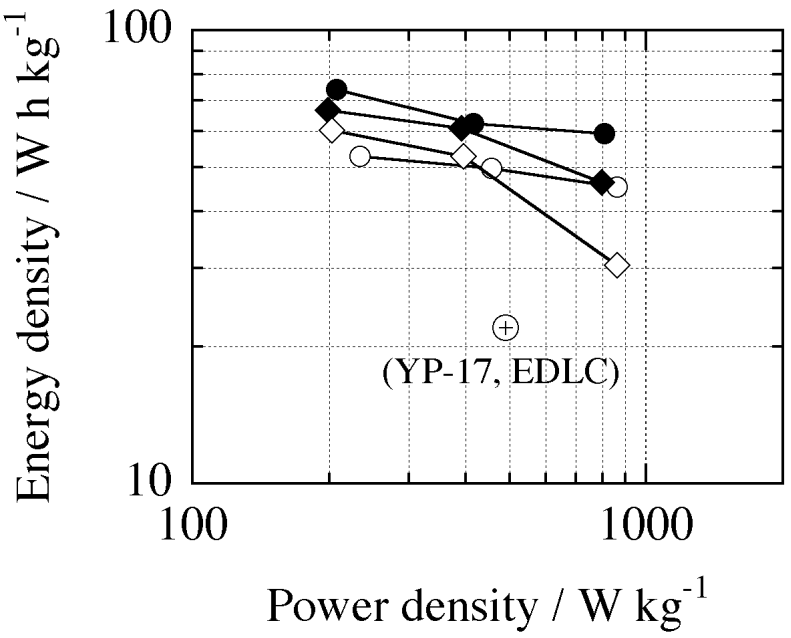
100
10
100
1000
Energy density / W h kg-1
Power density / W kg-1
(YP-17, EDLC)